

A 25 W 70% Efficiency Doherty Power Amplifier at 6 dB Output Back-Off for 2.4 GHz Applications with $V_{GS, PEAK}$ Control*

Amplificador de Potencia Doherty de 25 W, 70% de Eficiencia y Back Off de Salida de 6 dB para Aplicaciones a 2,4 GHz, con Control de $V_{GS, PEAK}$.

DOI:<http://dx.doi.org/10.17981/ingecuc.11.1.2015.04>

Research Article - Reception Date: August 30, 2014 - Acceptance Date: December 16, 2014

Jorge Moreno Rubio

Doctor of Electronic Devices, Universidad Pedagógica y Tecnológica de Colombia (Sogamoso). jorgejulian.moreno@uptc.edu.co

Edison Angarita Malaver

Master in Electronic Engineering, Universidad Pedagógica y Tecnológica de Colombia (Sogamoso). edison.angarita@uptc.edu.co

Herman Fernández González

Doctor of Information, Communication, and Computer Technologies, Universidad Pedagógica y Tecnológica de Colombia (Sogamoso). herman.fernandez@uptc.edu.co

To cite this paper:

Moreno Rubio, J., Angarita Malaver, E. y Fernández González, H., "Diseño y Simulación de un Amplificador de Potencia Doherty de 25 W con 70% de Eficiencia y Back Off de Salida de 6 dB para Aplicaciones a 2,4 GHz con Control de $V_{GS, PEAK}$ ", INGE CUC, 11 (1), 48-52, 2015. DOI: <http://dx.doi.org/10.17981/ingecuc.11.1.2015.04>

PEAK", INGE CUC, 11 (1), 48-52, 2015. DOI: <http://dx.doi.org/10.17981/ingecuc.11.1.2015.04>

Abstract— This paper shows the design and simulation results of a hybrid Doherty power amplifier. The amplifier has been designed at 2.4 GHz, obtaining power-added efficiency above 70 % for 6 dB output power back-off, together with a small signal gain of 17 dB. Design and analysis equations are presented considering class AB bias conditions for the main amplifier and class C for the peak one in back-off larger than 6 dB, and FET device assumption. An additional control on the bias point of the peak device has been carried out, in order to increase the gain on the Doherty region and ease the design of the peak branch. A Cree's GaN-HEMT CGH40010F device has been used with a nonlinear model guaranteed up to 6 GHz and with an expected output power of 10 W. The obtained output power is higher than 25-W. The simulation has been carried out using Agilent ADS CAD tools. The present design could present the state of the art in terms of continuous-wave (CW) characterization.

Key Words-- Power Amplifier, High Efficiency, GaN Devices, Doherty, Microwave Circuits.

Resumen-- Este artículo muestra el diseño y los resultados de simulación de un amplificador de potencia Doherty sobre tecnología híbrida. El amplificador fue diseñado a 2,4 GHz, obteniendo una eficiencia de potencia aditiva arriba del 70 % a 6-dB debajo de saturación, junto con una ganancia a pequeña señal de 17 dB. Las ecuaciones de análisis y diseño son presentadas considerando polarización clase AB para el amplificador principal y clase C para el amplificador auxiliar a 6-dB debajo de saturación, y dispositivos FET. Un control adicional sobre el punto de polarización del dispositivo auxiliar se ha llevado a cabo, para incrementar la ganancia en la región Doherty y facilitar el diseño de la rama auxiliar. Un dispositivo GaN-HEMT CGH40010 de Cree ha sido usado con un modelo no-lineal garantizado hasta 6-GHz y con una potencia de salida esperada de 10-W. La potencia de salida obtenida es mayor a 25-W. La simulación ha sido llevada a cabo usando Agilent ADS. El presente diseño representaría el estado del arte en términos de caracterización de onda continua (OC).

Palabras claves-- Amplificador de potencia, alta eficiencia, dispositivos GaN, Doherty, circuitos de microondas.

* Research paper deriving from the research Project "Implementación de estrategias para el manejo eficiente de la energía en transmisores aplicados a sistemas de comunicaciones inalámbricas". Funded by Grupo de Investigación en Telecomunicaciones (GINTEL) de la Universidad Pedagógica y Tecnológica de Colombia. Starting date: February 2014. Ending date: November 2015.

I. INTRODUCTION

The modulated signals driving the power amplifier in a modern wireless communication system transmitter are typically characterized by their high Peak-to-Average Power Ratio -PAPR. An example of this is the Universal Mobile Telecommunications System -UMTS, a Wideband Code Division Multiple Access -WCDMA standard application with PAPR ranging from 3 dB to more than 10 dB [1].

In Fig. 1, a typical simplified block scheme of a transmitter in a wireless communication system is shown. The function of the Power Amplifier (PA) is to increase the power of the modulated signal in order to be transmitted by the antenna. A single stage PA has an efficiency that is maximized just in saturation [2], [3]. Accordingly, the PA exploits its maximum efficiency only when the modulated signal presents the maximum amplitude. But, most of the time, the PA works in a large region of output power back-off, leading to very poor average efficiency [4] even if the PA presents a very high efficiency in saturation. Fig. 2 shows an example of typical distribution in power generation and efficiency as functions of output power in a single stage PA, for the sake of comparison.

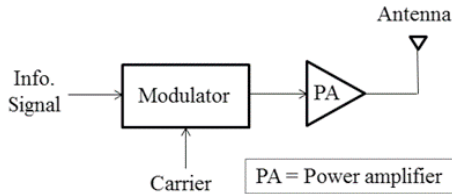


Fig. 1. Simplified block scheme of a transmitter in a wireless communication system. Source: Authors.

In order to increase the average efficiency, which means a lower transmission cost and avoiding energy loss, the Doherty Power Amplifier (DPA) [5] appears as one of the most common solutions [6] due to its simplicity when compared to others. In fact, a DPA keeps a maximized efficiency in a large output back-off as shown in Fig. 3.

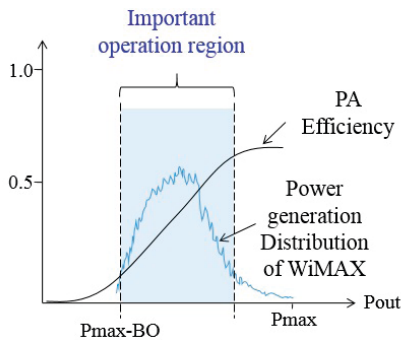


Fig. 2. Typical distribution in power generation and efficiency in a single stage PA vs. P_{out} output power. Source: Authors.

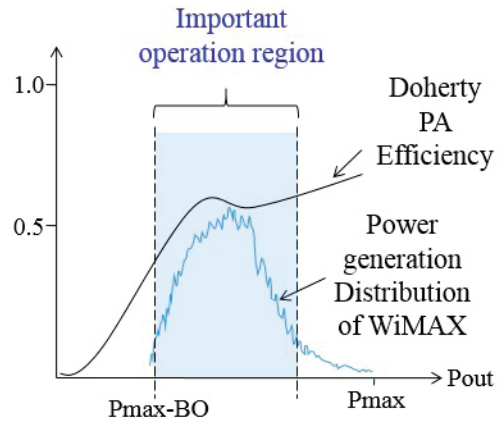


Fig. 3. Typical distribution in power generation and efficiency in a DPA. Source: Authors.

This paper shows the design of a DPA with 6 dB output back-off -OBO, using a GaN HEMT CGH40010 device (the same for main and peak amplifiers) with more than 20 W of output power. The second harmonic tuning -2nd HT method [3], has been performed at main and peak amplifiers in order to increase the efficiency on the Doherty region, which ranges from OBO to saturation. Also, a control over the gate voltage (VGS,PEAK) of the peak device has been included. An RF35 substrate from Taconic Company has been used together with an ADS (Advanced Design System) as simulation tool. The second section of this paper presents a general explanation of the Doherty Power Amplifier concept; the third section shows the design strategy that has been carried out in this work. Finally, the results obtained and conclusions are presented in sections IV and V respectively.

II. DOHERTY POWER AMPLIFIER CONCEPT

The general DPA scheme is shown in Fig. 4, in order to explain its behavior. In terms of efficiency, three power regimes are taken into account; these are: low power, Doherty and saturation regions.

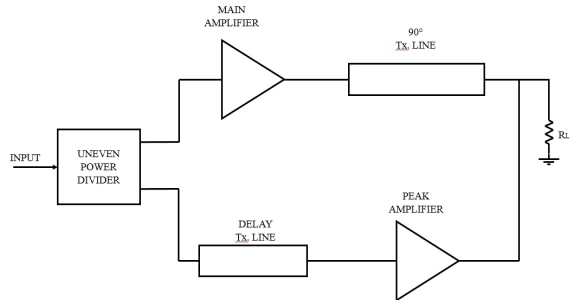


Fig. 4. General scheme of a DPA. Source: Authors.

At the low power region, the main amplifier is on, whereas the peak amplifier is totally off. In this way, no current is injected to the common load R_L from the peak amplifier, which has an output reflection coefficient of $S_{22}=1$, therefore, the load for the main $R_{M,LP}$ is given by the transformation of the common load through the Z_0 impedance inverter -90 degrees transmission line in Fig. 4; this means

$$R_{M,P} = \frac{Z_0^2}{R_L} \quad (1)$$

The value given by (1) for the characteristic impedance Z_0 is equal to the real optimal load for the main amplifier R_{opt} , while the common load R_L is typically a half of it for a 6 dB OBO, considering the same device for main and peak amplifiers, as shown in [3]. Thus, the resulting value of $R_{M,LP}$ is shown by (2):

$$R_{M,P} = 2Z_0 = 2R_{opt} \quad (2)$$

Increasing the input power, the dynamic load line for the main device “grows up” until reaching the knee voltage V_k ($P_{out}=P_{sat}-OBO$) constraint, as shown in Fig. 5. At this point, called “break point”, the main amplifier will reach its maximum drain efficiency, and at the same time, it will be the whole DPA’s efficiency because the peak device is off.

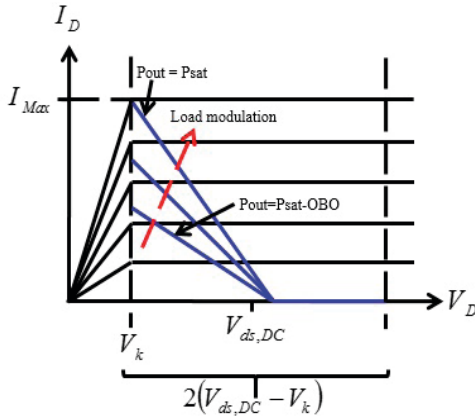


Fig. 5. Load modulation for a typical DPA.
Source: Authors.

After the break point, if the input power is continuously increased, the peak amplifier turns on. Therefore, a current is injected to the common load from the peak amplifier producing load modulation for the main device, as represented in Fig. 5 by the dotted arrow. In other words, the dynamic load line slope increases with the input power. At that moment, the DPA efficiency will be given by

the weighted efficiency of the main and peak amplifiers. The current’s phase from main and peak amplifiers must be equal at the common load node (combining point).

Finally, with the input power increase, the load line of the main amplifier also reaches its maximum current limitation $I_{Max,m}$ (see Fig. 5). Here, the complete saturation of the DPA occurs. The expected drain efficiency η (%) is shown in Fig. 6, as a function of the output power.

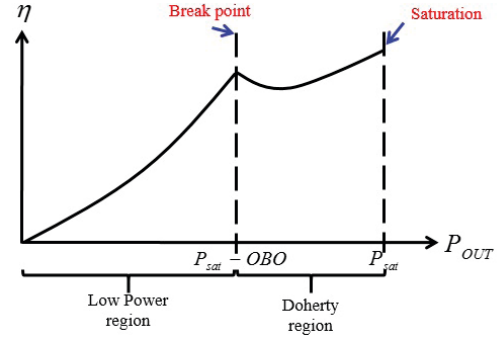


Fig. 6. Efficiency vs output power for a Doherty power amplifier.
Source: Authors.

III. DOHERTY POWER AMPLIFIER DESIGN

A Cree’s GaN CGH40010F device has been selected accordingly with the advantage in power delivered by this kind of devices [7]. In this case, a cold FET simulation [8] has been carried out in order to extract the device’s drain-source capacitance and the parasites due to the package, allowing the identification of the device’s intrinsic drain (see Fig. 7). Therefore, the output matching network must be designed to produce the real optimal load in the intrinsic drain of the device. In Fig. 7, L_{OUT} and C_{OUT} provide an approximation of the equivalent output parasite network (C_{OUT} includes the C_{DS} effect).

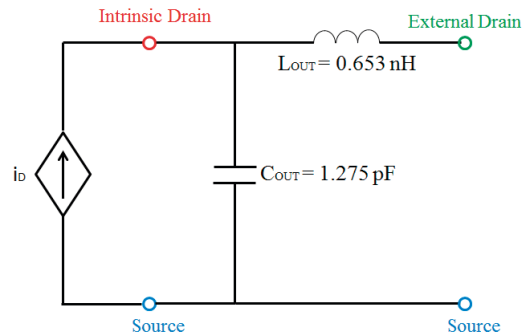


Fig. 7. Intrinsic drain identification for the GaN device.
Source: Authors.

As main branch, an inverse class F amplifier has been designed. In this case, the inverse class F configuration has been considered as a second harmonic tuned one [3].

On the other hand, the peak amplifier is just a replica of the main one, but the bias point is controlled depending on the power regime. In other words, at 6 dB OBO the peak amplifier is a deep class C power amplifier, while at 0 dB OBO, its bias point is changed to be identical to the main amplifier's one. This has been carried out by increasing, in a linear way, the gate's DC voltage in the peak device ($V_{GS,PEAK}$) from -6V to -2.73V. The initial value $V_{GS,PEAK} = -6$ V is selected using the trans-conductance method as shown in [3].

The control on VGS for the peak branch elevates the total gain on the Doherty region in comparison with one without this kind of control [9], [10]. In other words, the conduction angle of the peak device is increased up to reach the same as the main device. Therefore, given that the fundamental drain current for both main and peak amplifiers must be the same in saturation, the peak amplifier can be exactly identical to the main one. In addition, in saturation, main and peak amplifiers have the same gain, accordingly a one-to-one input power ratio has to be implemented [11]. DC $V_{GS,PEAK}$ as a function of the output power is shown in Fig. 8.

The output matching networks –OMN of both amplifiers (main and peak) have been designed as shown in Fig. 9. The bias T is implemented using a $\lambda/4$ transmission line, which is also used in order to produce the second harmonic load at the intrinsic drain of the device -a very large magnitude load. At the fundamental frequency, the OMN is designed for compensating the equivalent output parasite network as presented in [10].

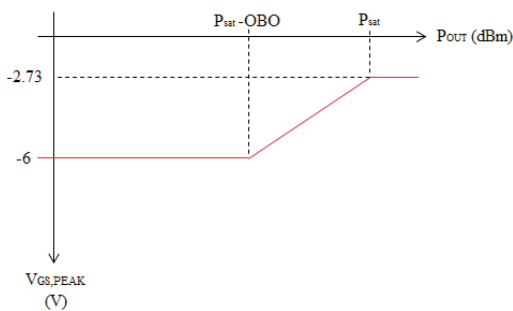


Fig. 8. Peak device DC gate-source voltage vs. output power. Source: Authors.

The input matching network –IMN has been designed for small signal matching. Also, a stabilization network is included at the input network to ensure unconditional stability at all frequencies. Fig. 10 shows the scheme of the designed IMN and the final scheme of the designed DPA is shown in Fig. 11.

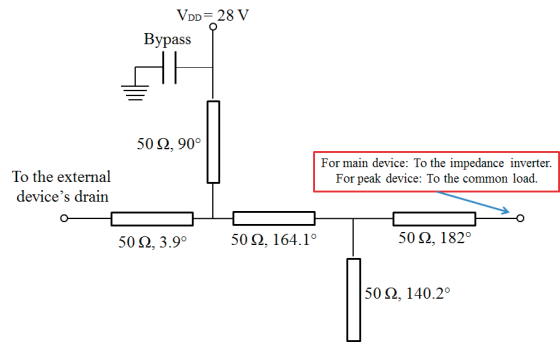


Fig. 9. Output matching network of both main and peak amplifiers. Source: Authors.

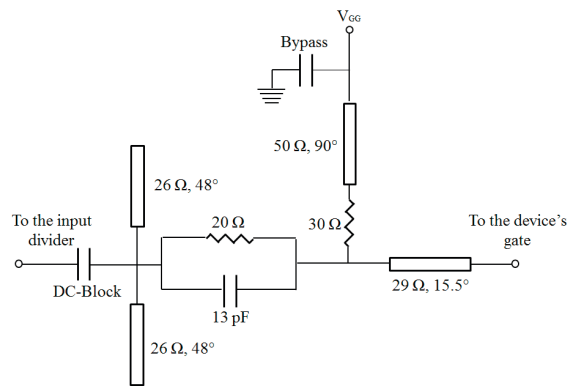


Fig. 10. Input matching network of both main and peak amplifiers. Source: Authors.

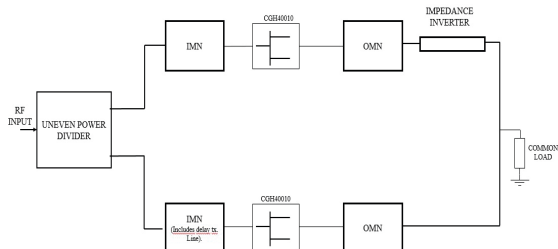


Fig. 11. Scheme of the designed DPA. Source: Authors.

IV. RESULTS

A simulation using Advanced Design System software is carried out in order to obtain the results. Gain and drain efficiency as a function of the output power P_{OUT} are shown in Fig. 12. As can be noticed, the obtained gain on the Doherty region is between 12.5 and 14 dB (AM/AM of 1.5 dB), and the power-added efficiency (PAE) is higher than 70%, whereas at saturation is 75%. A maximum output power of 45 dBm has been obtained as

well. These results are considered by the authors as being competitive with the state-of-art in terms of CW characterization. The implemented DPA is shown in Fig. 13. And currently it is waiting for a measurement run.

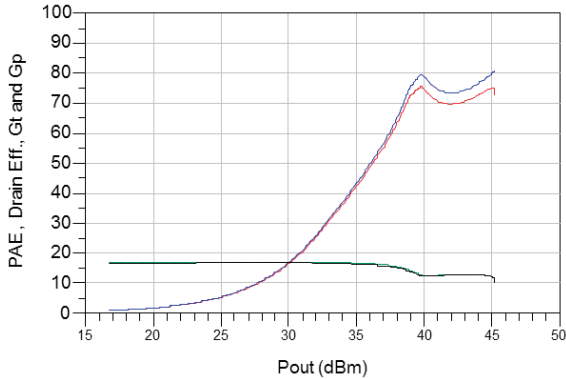


Fig. 12. PAE (% squares), Drain Efficiency (% circles), Transducer Gain G_t (dB stars) and Operation Gain G_p (dB diamonds) as function of Output Power P_{out} (dBm). Source: Authors.

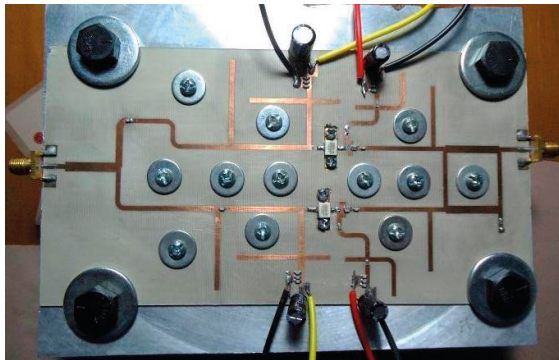


Fig. 13. Implemented circuit. Source: Authors.

V. FUNDS

This investigation was financed with resources from the Grupo de Investigación en Telecomunicaciones GINTEL of the Universidad Pedagógica y Tecnológica de Colombia under *RF/microwave Projects* program.

VI. CONCLUSION

A high efficiency Doherty Power Amplifier with controlled gate-voltage has been designed, obtaining more than 70% of power-added efficiency on Doherty region (6-dB) and 45 dBm of output power at 2.4 GHz. These performances place this amplifier in possible applications for systems operating in the 2.4 GHz band with high peak-to-average power ratios.

REFERENCES

- [1] J. Moreno, J. Fang, R. Quaglia, V. Camarchia, M. Pirola, and G. Ghione, "Development of single-stage and doherty GaN-based hybrid RF power amplifiers for quasi-constant envelope and high peak to average power ratio wireless standards," *Microw. Opt. Technol. Lett.*, vol. 54, no. 1, pp. 206–210, 2012. DOI:10.1002/mop.26459
- [2] S. Cripps, *RF Power Amplifiers for Wireless Communications*, 2nd ed. Norwood: Artech House, 2006.
- [3] P. Colantonio, F. Giannini, and E. Limiti, *High Efficiency RF and Microwave Solid State Power Amplifiers*, 1st ed. Gran Bretaña: Wiley, 2009.
- [4] K. Bumman, M. Junghwan, and K. Ildu, "Efficiently Amplified," *IEEE Microw. Mag.*, vol. 11, no. 5, pp. 87–100, 2010. DOI:10.1109/MMM.2010.937099
- [5] W. Doherty, "A New High Efficiency Power Amplifier for Modulated Waves," *IEEE RFIC Virtual J.*, vol. 24, no. 1, pp. 1163–1182, 2006. DOI:10.1109/JRPROC.1936.228468
- [6] B. Kim, I. Kim, and J. Moon, "Advanced Doherty Architecture," *IEEE Microw. Mag.*, vol. 11, no. 5, pp. 72–86, 2010. DOI:10.1109/MMM.2010.937098
- [7] J. Shealy, J. Smart, M. Poulton, R. Sadler, D. Grider, S. Gibb, B. Hosse, B. Sousa, D. Halchin, and V. Steel, "Gallium nitride (GaN) HEMT's: Progress and potential for commercial applications," in *Symposium Gallium Arsenide Integrated Circuit (GaAs IC)*, 2002, pp. 243–246. DOI:10.1109/gaas.2002.1049069
- [8] J. Lu, Y. Wang, L. Ma, and Z. Yu, "A new small-signal modeling and extraction method in AlGaIn/GaN HEMT's," *Solid. State. Electron.*, vol. 52, no. 1, pp. 115–120, 2008. DOI:10.1016/j.sse.2007.07.009
- [9] J. Rubio, J. Fang, R. Quaglia, V. Camarchia, M. Pirola, S. Guerrieri, and G. Ghione, "A 22W 65% efficiency GaN Doherty Power Amplifier at 3.5 GHz for WiMAX applications," in *Workshop on Integrated Nonlinear Microwave and Millimetre-Wave Circuits (INMMIC)*, 2011, pp. 1–4. DOI:10.1109/inmmic.2011.5773332
- [10] J. Rubio, J. Fang, R. Quaglia, V. Camarchia, M. Pirola, S. Guerrieri, and G. Ghione, "'3-3.6-GHz Wideband GaN Doherty Power Amplifier Exploiting Output Compensation Stages," *IEEE Trans. Microw. Theory Tech.*, vol. 60, no. 8, pp. 2543–2548, 2012. DOI:10.1109/TMTT.2012.2201745
- [11] V. Camarchia, J. Fang, J. Moreno Rubio, M. Pirola, and R. Quaglia, "7 GHz MMIC GaN Doherty Power Amplifier With 47% Efficiency at 7 dB Output Back-Off," *IEEE Microw. Wirel. Components Lett.*, vol. 23, no. 1, pp. 34–36, 2012. DOI:10.1109/LMWC.2012.2234090